

# Direct Synthesis of Nitriles from Aldehydes and Hydroxylamine Hydrochloride Catalyzed by a HAP@AEPH<sub>2</sub>-SO<sub>3</sub>H Nanocatalyst

Samane Memar Masjed,<sup>A</sup> Batool Akhlaghinia,<sup>A,B</sup> Monireh Zarghani,<sup>A</sup> and Nasrin Razavi<sup>A</sup>

<sup>A</sup>Department of Chemistry, Faculty of Sciences, Ferdowsi University of Mashhad, Mashhad 9177948974, Iran.

<sup>B</sup>Corresponding author. Email: akhlaghinia@um.ac.ir

We describe an efficient method for the direct preparation of nitriles from aldehydes and hydroxylamine hydrochloride catalyzed by sulfonated nanohydroxyapatite functionalized by 2-aminoethyl dihydrogen phosphate (HAP@AEPH<sub>2</sub>-SO<sub>3</sub>H) as an eco-friendly and recyclable solid acid nanocatalyst. In this protocol the use of a solid acid nanocatalyst provides a green, useful, and rapid method for the preparation of nitriles in excellent yields. In addition, the notable feature of this methodology is that the synthesized nanocatalyst can be recovered and reused five times without any noticeable loss of efficiency.

Manuscript received: 2 March 2016.

Manuscript accepted: 15 May 2016.

Published online: 14 June 2016.

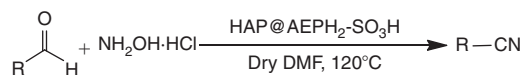
## Introduction

Nitriles, as a key constituent in various natural products, are important starting materials in chemical and pharmaceutical industries, and have been widely used in the production of valuable compounds such as polymers, agrochemicals, pharmaceuticals, and dyes.<sup>[1]</sup> In addition, they serve as useful precursors in the synthesis of many magnificent functional compounds such as amides,<sup>[2]</sup> carboxylic acids,<sup>[3]</sup> amines,<sup>[4]</sup> ketones,<sup>[5]</sup> esters,<sup>[6]</sup> and heterocycles.<sup>[7]</sup> Up to now, a large number of synthetic protocols for the preparation of nitriles have been developed, including the hydrocyanation of alkenes,<sup>[8]</sup> the Sandmeyer reaction of diazonium salts,<sup>[9]</sup> the Rosenmund–von Braun reaction of aryl halides,<sup>[10]</sup> and the Kolbe nitrile synthesis.<sup>[11]</sup> Other alternative methods for the synthesis of these compounds involve the one-step conversion of aldehydes into nitriles, which is one of the most efficient and cleanest routes for this transformation.<sup>[12]</sup> During the past decades, studies on the preparation of nitriles from aldehydes have received much attention and several methods are reported in the literature, which include using trichloroisocyanuric acid (TCCA),<sup>[13]</sup> dry alumina,<sup>[14]</sup> FeCl<sub>3</sub>,<sup>[15]</sup> graphite,<sup>[16]</sup> zinc oxide (ZnO),<sup>[17]</sup> Ag nanoparticles (NPs),<sup>[18]</sup> [BMIM(SO<sub>3</sub>H)][OTf] (BMIM = 1-butyl-3-methyl-imidazolium),<sup>[19]</sup> aceto-hydroxamic acid/Bi(OTf)<sub>3</sub>,<sup>[20]</sup> CuO NPs,<sup>[21]</sup> CeCl<sub>3</sub>·7H<sub>2</sub>O/KI/H<sub>2</sub>O<sub>2</sub>,<sup>[22]</sup> triflic acid,<sup>[23]</sup> and electrochemical methods.<sup>[24]</sup> However, earlier synthetic methods suffered from one or more of the following drawbacks: the use of strong acids or bases or oxidants, prolonged reaction time, low yield, requirement of excess reagents/catalysts, laborious work-up procedures, or harsh reaction conditions. Thus,

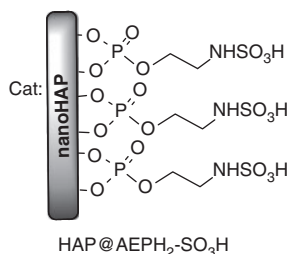
the development of a simple, highly efficient, and catalytic process is still in great demand.

In recent years, solid acid catalysts, which play a significant role in the development of clean technologies, have attracted increasing interest and been successfully used in a variety of catalytic reactions.<sup>[25]</sup> As compared with traditional liquid acids, solid acid catalysts have many advantages such as efficiency, operational simplicity, easy recyclability, non-corrosive nature, and environmental friendliness. To the best of our knowledge, the employment of solid acids in the synthesis of nitriles has been poorly exploited in the past.<sup>[26]</sup> So it is of great practical importance to develop a more efficient and environmentally benign method for this synthesis.

Previously, we successfully synthesized sulfonated nanohydroxyapatite functionalized by 2-aminoethyl dihydrogen phosphate (HAP@AEPH<sub>2</sub>-SO<sub>3</sub>H) as a new, green heterogeneous nanocatalyst by modification of nanohydroxyapatite with 2-aminoethyl dihydrogen phosphate (AEPH<sub>2</sub>) (as a new bifunctional organic molecule) and then sulfonating with chlorosulfonic acid.<sup>[27]</sup> The catalytic activity of the synthesized nanocatalyst was initially used for the synthesis of 4,4'-(aryl methylene)bis(1*H*-pyrazol-5-ol) derivatives with good to excellent yields. After that, the catalytic use of the HAP@AEPH<sub>2</sub>-SO<sub>3</sub>H nanocatalyst was extended to the direct esterification of carboxylic acids with alcohols.<sup>[28]</sup> As expected, the desired products (esters) were obtained in high yields. So, prompted by these findings and in continuation of our studies on the development of novel and efficient heterogeneous catalysts in the synthesis of organic compounds,<sup>[29]</sup>



R = C<sub>6</sub>H<sub>4</sub>, 4-(OH)C<sub>6</sub>H<sub>4</sub>, 2-(OH)C<sub>6</sub>H<sub>4</sub>, 4-(OMe)C<sub>6</sub>H<sub>4</sub>, 3-(OMe)C<sub>6</sub>H<sub>4</sub>, 4-(OEt)C<sub>6</sub>H<sub>4</sub>, 4-(Me)C<sub>6</sub>H<sub>4</sub>, 2-MeC<sub>6</sub>H<sub>4</sub>, 4-(<sup>t</sup>Pr)C<sub>6</sub>H<sub>4</sub>, 4-(Me<sub>2</sub>N)C<sub>6</sub>H<sub>4</sub>, 4-(Cl)C<sub>6</sub>H<sub>4</sub>, 2,6-(Cl)<sub>2</sub>C<sub>6</sub>H<sub>3</sub>, 4-(Br)C<sub>6</sub>H<sub>4</sub>, 4-(NO<sub>2</sub>)C<sub>6</sub>H<sub>4</sub>, 4-(CN)C<sub>6</sub>H<sub>4</sub>, 2-pyridyl, 3-pyridyl, 2-Thiophene, 1-naphthyl, CH<sub>3</sub>(CH<sub>2</sub>)<sub>3</sub>CH<sub>2</sub>, CH<sub>3</sub>(CH<sub>2</sub>)<sub>6</sub>CH<sub>2</sub>, (CH<sub>3</sub>)<sub>2</sub>CH-CH<sub>2</sub>.



**Scheme 1.** Direct preparation of nitriles from aldehydes and hydroxylamine hydrochloride catalyzed by HAP@AEPH<sub>2</sub>-SO<sub>3</sub>H nanocatalyst.

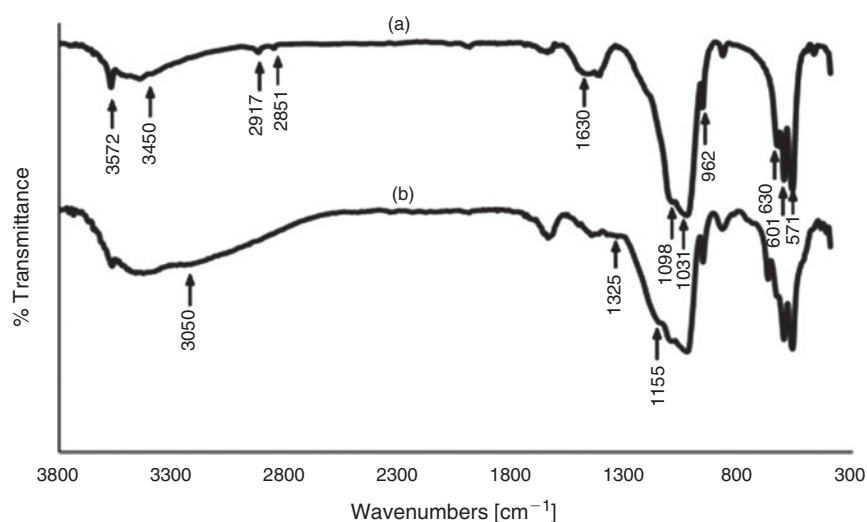


**Fig. 1.** FT-IR spectrum of (a) HAP@AEPH<sub>2</sub> and (b) HAP@AEPH<sub>2</sub>-SO<sub>3</sub>H.

herein, we report the application of HAP@AEPH<sub>2</sub>-SO<sub>3</sub>H as a reusable solid acid nanocatalyst to the efficient synthesis of nitriles from aldehydes and hydroxylamine hydrochloride (Scheme 1).

## Results and Discussion

### Characterization of the Nanocatalyst

The HAP@AEPH<sub>2</sub>-SO<sub>3</sub>H nanocatalyst was synthesized according to the procedure reported in our previous study.<sup>[27]</sup> The structure and morphology of the prepared nanocatalyst was characterized by the following techniques: FT-IR spectroscopy, X-ray powder diffraction (XRD), scanning electron microscopy (SEM), transmission electron microscopy (TEM), thermogravimetric analysis (TGA), differential thermal analysis (DTA), elemental analysis (CHN), and Brunauer–Emmett–Teller (BET) surface area analysis which confirmed the successful preparation of the new nanocatalyst.<sup>[27,28]</sup>

The FT-IR spectra of HAP@AEPH<sub>2</sub> and HAP@AEPH<sub>2</sub>-SO<sub>3</sub>H are shown in Fig. 1. As can be seen from Fig. 1a, the stretching and bending vibrations of the OH<sup>-</sup> ion in hydroxyapatite were detected around 3572 and 630 cm<sup>-1</sup> respectively. Also, the broad band at 3450–3050 cm<sup>-1</sup> (due to stretching vibration) and the weak band at 1637–1630 cm<sup>-1</sup> (due to bending vibration) were attributed to the crystal water and surface adsorbed water. Additional vibrational modes at 1098, 1031, 962, 601, 571, and 471 cm<sup>-1</sup> could be ascribed to the asymmetric, symmetric stretching, and bending vibrations of the PO<sub>4</sub><sup>3-</sup> ions respectively.<sup>[30]</sup> Successful functionalization of the nanoHAP with AEPH<sub>2</sub> was evidenced by the absorption bands at 2917 and 2851 cm<sup>-1</sup> due to the asymmetric and symmetric vibrational frequencies of -CH<sub>2</sub> (Fig. 1a).<sup>[31]</sup> In the FT-IR spectrum of HAP@AEPH<sub>2</sub>-SO<sub>3</sub>H (Fig. 1b), the intensity of the absorption band at 3450–3050 cm<sup>-1</sup> was increased because of the presence of more OH groups which appeared after sulfonation. In addition, two new absorption bands appeared

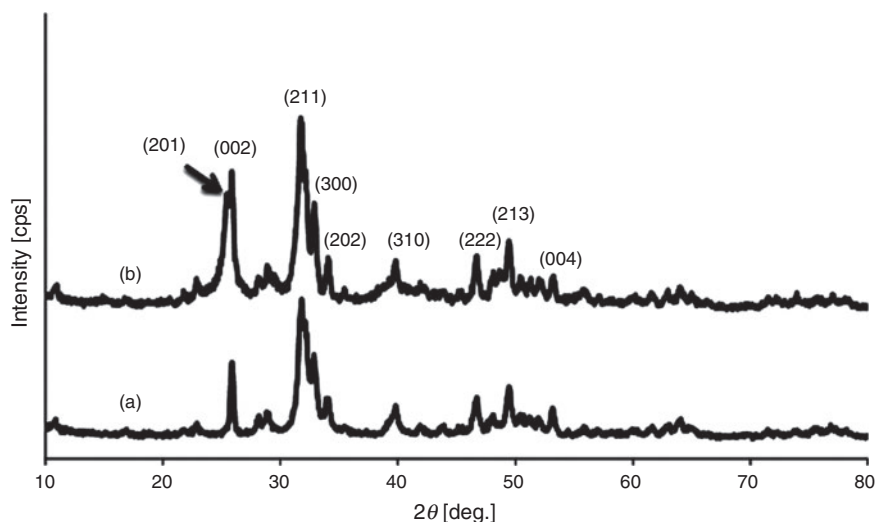


Fig. 2. The XRD patterns of (a) HAP@AEPH<sub>2</sub> and (b) HAP@AEPH<sub>2</sub>-SO<sub>3</sub>H.

at 1325 and 1155 cm<sup>-1</sup>, which were ascribed to the asymmetric and symmetric stretching frequencies of S=O.<sup>[32]</sup> These results revealed that the modified nanoHAP were functionalized by -SO<sub>3</sub>H groups successfully.

XRD measurements were used to identify the crystalline structure of HAP@AEPH<sub>2</sub> and HAP@AEPH<sub>2</sub>-SO<sub>3</sub>H. As shown in Fig. 2, characteristic peaks ((002), (211), (300), (202), (310), (222), (213) and (004)) were observed for both samples. These peaks are consistent with the JCPDS file (PDF No. 74-0565)<sup>[33]</sup> and reveal that the resultant nanoparticles were nanoHAP with a hexagonal phase. It is also observed that the modification of the nanoHAP with AEPH<sub>2</sub> and chlorosulfuric acid did not result in a phase change of the nanoHAP.

Although XRD analysis of the HAP@AEPH<sub>2</sub>-SO<sub>3</sub>H showed no considerable broadening or shifting of peaks when compared with the XRD of HAP@AEPH<sub>2</sub> (Fig. 2), an additional peak observed in the HAP@AEPH<sub>2</sub>-SO<sub>3</sub>H pattern at 2θ = 25.4° could be attributed to a small impurity of CaSO<sub>4</sub> due to sulfonation (JCPDS: 37-1496) (Fig. 2b).<sup>[34]</sup>

SEM and TEM were used to obtain direct information about the structure and morphology of the HAP@AEPH<sub>2</sub>-SO<sub>3</sub>H NPs. From the SEM images shown in Fig. 3a, b, HAP@AEPH<sub>2</sub>-SO<sub>3</sub>H NPs have a uniform nanorod morphology which is similar to the particle morphology reported elsewhere.<sup>[35]</sup> In addition, Fig. 3c, d show the TEM images of the HAP@AEPH<sub>2</sub>-SO<sub>3</sub>H NPs. It was found that the synthesized NPs are rod in shape with a mean size range of 10–100 nm. Obviously, there was no essential change in the nanoHAP morphology after being functionalized with AEPH<sub>2</sub> and sulfonic acid.<sup>[36]</sup>

TGA of the nanoparticles was also used to determine the content of organic functional groups of the sample (Fig. 4). For HAP@AEPH<sub>2</sub>, weight loss at temperatures below 200°C (4.00 %) is attributed to the physically adsorbed water on the catalyst surface. Also, the weight loss of the nanocatalyst in the range of 200 to 500°C is related to the thermal decomposition of AEPH<sub>2</sub> anchored on the surface of nanoHAP (Fig. 4a).<sup>[37]</sup> The TGA thermogram of HAP@AEPH<sub>2</sub>-SO<sub>3</sub>H (Fig. 4b) shows three weight loss steps. The initial weight loss up to 200°C is due to absorbed water, the second step involves the decomposition of AEPH<sub>2</sub> which started after 200°C and continued up to 500°C. The last step can be observed between 500 and 850°C, corresponding to the thermal decomposition of SO<sub>3</sub>H groups

embedded via AEPH<sub>2</sub> on the surface of nanoHAP.<sup>[38]</sup> From the change of weight percentage in the TGA thermogram, it can be estimated that the amount of AEPH<sub>2</sub> and sulfonic acid functionalized into the surface of the catalyst are ~5.60 and 8.00 % respectively.

In addition to structural confirmation and TGA, quantitative determination of AEPH<sub>2</sub> and sulfonic acid onto the surface of nanoHAP were performed by elemental analysis (Table 1). The elemental analysis of the catalyst showed that 1.008 mmol of AEPH<sub>2</sub> and 1.040 mmol of sulfonic acid are incorporated into 1.000 g of HAP@AEPH<sub>2</sub>-SO<sub>3</sub>H. Notably, the obtained results from elemental analysis of the nanocatalyst are in good agreement with the results obtained from TGA.

The amount of acidic sites in HAP@AEPH<sub>2</sub>-SO<sub>3</sub>H was also determined by back-titration analysis of the catalyst: 100 mg of catalyst was added to a solution of NaOH (15 mL, 0.1 N). The resulting suspension was maintained at room temperature overnight under stirring. After that, the suspension was filtered. The filtrate was neutralized by a standard solution of HCl (0.1 M). The consumed volume of HCl (14.1 mL) determined the amount of loaded NHSO<sub>3</sub>H per 1.000 g of HAP@AEPH<sub>2</sub>-SO<sub>3</sub>H (0.900 mmol of NHSO<sub>3</sub>H per 1.000 g of nanocatalyst). This result is in good agreement with those of the results obtained from TGA and elemental analysis.

The nitrogen adsorption–desorption isotherm of the HAP@AEPH<sub>2</sub>-SO<sub>3</sub>H demonstrates the average surface area, pore volume, and pore size of the HAP@AEPH<sub>2</sub>-SO<sub>3</sub>H. In comparison with the literature, the surface area of HAP@AEPH<sub>2</sub>-SO<sub>3</sub>H is a little smaller than the pure HAP NPs (Table 2).<sup>[39]</sup>

#### Catalytic Synthesis of Nitriles

In continuation of our recent studies on the application of the HAP@AEPH<sub>2</sub>-SO<sub>3</sub>H nanocatalyst in the development of useful synthetic methodologies,<sup>[27,28]</sup> we now show a protocol that uses HAP@AEPH<sub>2</sub>-SO<sub>3</sub>H as a green and efficient solid acid nanocatalyst for direct preparation of nitriles from aldehydes and hydroxylamine hydrochloride (Scheme 1). In an endeavour to start our present investigation, the reaction of 4-methoxybenzaldehyde and hydroxylamine hydrochloride (NH<sub>2</sub>OH·HCl) was chosen as a model reaction for optimizing the reaction conditions (Table 3).

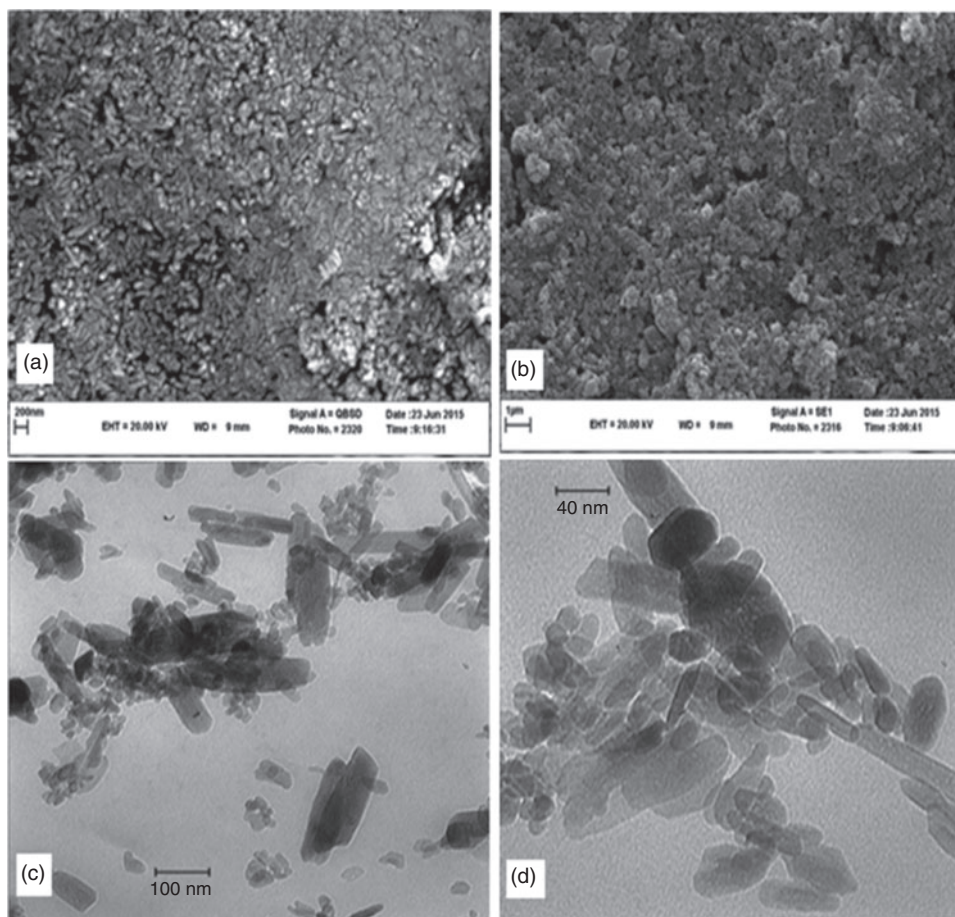


Fig. 3. (a, b) SEM images of HAP@AEPH<sub>2</sub>-SO<sub>3</sub>H. (c, d) TEM images of HAP@AEPH<sub>2</sub>-SO<sub>3</sub>H.

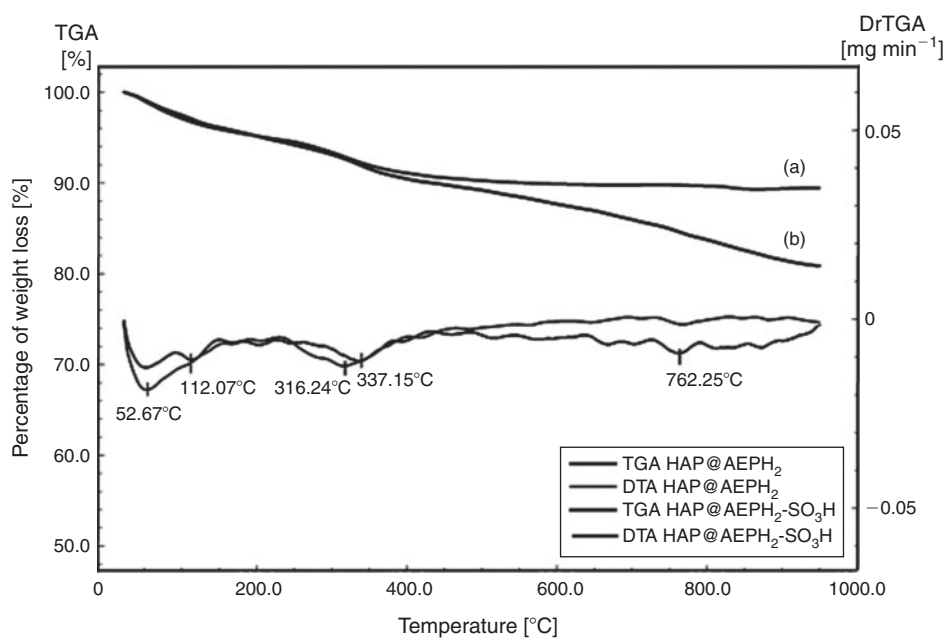


Fig. 4. The TGA/DTA thermograms of (a) HAP@AEPH<sub>2</sub> and (b) HAP@AEPH<sub>2</sub>-SO<sub>3</sub>H.

In the absence of any catalyst at 120°C, no reaction occurred after 24 h (Table 3, entry 1), while 4-methoxybenzonitrile can be obtained in 98% yield when 8 mol-% of HAP@AEPH<sub>2</sub>-SO<sub>3</sub>H was used as catalyst (Table 3, entry 2). The role of

HAP@AEPH<sub>2</sub>-SO<sub>3</sub>H as a solid acid nanocatalyst has been further confirmed when a similar reaction was carried out in the presence of HAP NPs and HAP@AEPH<sub>2</sub> NPs (Table 3, entries 3 and 4). It was observed that the desired product was

**Table 1.** TGA and elemental analysis data of HAP@AEPH<sub>2</sub> and HAP@AEPH<sub>2</sub>-SO<sub>3</sub>H

Samples	TGA [% (mmol g <sup>-1</sup> )]			Elemental analysis [w/w % (mmol g <sup>-1</sup> )]		
	H <sub>2</sub> O	AEPH <sub>2</sub>	SO <sub>3</sub> H	C	N	S
HAP@AEPH <sub>2</sub>	4.000 (2.200)	5.600 (1.010)	–	2.409 (1.004)	1.397 (1.000)	–
HAP@AEPH <sub>2</sub> -SO <sub>3</sub> H	4.000 (2.200)	5.600 (1.010)	8.000 (1.065)	2.419 (1.008)	1.409 (1.007)	3.32 (1.040)

**Table 2.** BET surface area, pore volume and pore size of HAP@AEPH<sub>2</sub>-SO<sub>3</sub>H

Sample	Morphology	S <sub>BET</sub> [m <sup>2</sup> g <sup>-1</sup> ]	Pore volume [cm <sup>3</sup> g <sup>-1</sup> ]	Pore size [nm]
HAP@AEPH <sub>2</sub> -SO <sub>3</sub> H	Nanoparticle	130.2	0.391	12.011

**Table 3.** Direct conversion of 4-methoxybenzaldehyde into 4-methoxybenzoxime in the presence of HAP@AEPH<sub>2</sub>-SO<sub>3</sub>H nanocatalyst under different reaction conditions

Entry	Catalyst [mol-%]	Solvent	Molar ratio (4-methoxybenzaldehyde/NH <sub>2</sub> OH·HCl)	Temperature [°C]	Time [min]	Isolated yield [%]
1	–	DMF	1 : 5	120	24 h	20
2	8	DMF	1 : 5	120	45	98
3 <sup>A</sup>	8	DMF	1 : 5	120	24	40
4 <sup>B</sup>	8	DMF	1 : 5	120	24	40
5	10	DMF	1 : 5	120	40	98
6	6	DMF	1 : 5	120	45	70
7	8	DMF	1 : 5	110	45	80
8	8	DMF	1 : 4	120	45	98
9	8	DMF	1 : 3	120	45	98
10	8	DMF	1 : 2	120	45	80
11	8	DMSO	1 : 3	120	2 h	20
12	8	H <sub>2</sub> O	1 : 3	Reflux	8 h	70
13	8	THF	1 : 3	Reflux	4 h	75
14	8	CH <sub>3</sub> CN	1 : 3	Reflux	2 h	50
15	8	CH <sub>2</sub> Cl <sub>2</sub>	1 : 3	Reflux	9 h	30

<sup>A</sup>The reaction was performed in the presence of HAP NPs.

<sup>B</sup>The reaction was performed in the presence of HAP@AEPH<sub>2</sub> NPs.

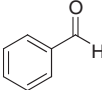
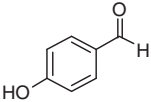
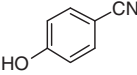
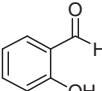
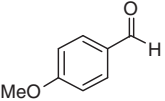
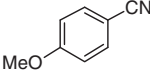
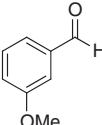
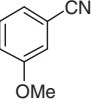
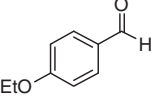
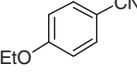
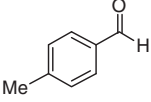
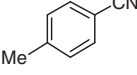
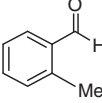
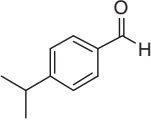
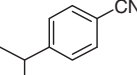
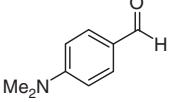
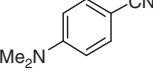
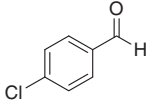
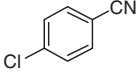
scarcely obtained (40%). In order to optimize the reaction conditions, different amounts of catalyst were first examined on the model reaction. As shown in Table 3, a further increase in the amount of catalyst has no significant effect on the yield or reaction time (Table 3, entry 5), whereas decreasing the amount of HAP@AEPH<sub>2</sub>-SO<sub>3</sub>H nanocatalyst led to a lower yield of the desired product (Table 3, entry 6). An attempt was also made to catalyse the reaction at lower temperature but the outcome was not promising (Table 3, entry 7). The effect of different molar ratios of 4-methoxybenzaldehyde/NH<sub>2</sub>OH·HCl on the reaction rate was also investigated. It can be seen that a decrease in molar ratio from 1 : 5 to 1 : 3 has no effect on the reaction yield (95%) (Table 3, entries 8, 9). However, reducing the molar ratio from 1 : 3 to 1 : 2 was accompanied by a considerable drop of yield (Table 3, entry 10). In addition, the reaction was carried out in different solvents. Among the various solvents tested, DMF was found to be the best solvent giving a maximum yield of the desired product in a short reaction time. As shown in Table 3, in the reactions employing DMSO, H<sub>2</sub>O, THF, CH<sub>3</sub>CN, and CH<sub>2</sub>Cl<sub>2</sub> as solvents, the reactions did not progress efficiently and low yields of the corresponding product were obtained even after a long reaction time (Table 3, entries 11–15).

Consequently, the optimal reaction conditions have been identified: applying a 1 : 3 molar ratio of 4-methoxybenzaldehyde/NH<sub>2</sub>OH·HCl at 120°C, in the presence of 8 mol-% HAP@AEPH<sub>2</sub>-SO<sub>3</sub>H nanocatalyst.

Encouraged by our initial studies, we next explored the generality and scope of the protocol using a series of structurally different aldehydes under the optimized reaction conditions (Table 3, entry 9). The results are displayed in Table 4. From this table, it is clear that all reactions afforded the corresponding products in moderate to high yields irrespective of the electronic nature of the aldehydes (Table 4, entries 1–22). Aromatic aldehydes bearing an electron-donating group afford the corresponding products rapidly in high yields (Table 4, entries 2–10). In contrast, the reaction of aromatic aldehydes with electron withdrawing substituents such as –Cl, –Br, –NO<sub>2</sub>, and –CN, require longer reaction times to proceed properly (Table 4, entries 11–15). Moreover, it should be noted that the *ortho*-substituted aldehydes render lower yields (Table 4, entry 3, 8, 12) due to the steric hindrance. In our study, to expand the scope of this methodology, a series of hetero-arylaldehydes were employed to react with hydroxylamine hydrochloride under the optimized conditions. The desired products were obtained in

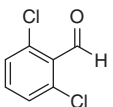
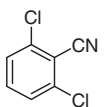
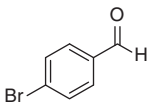
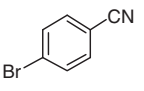
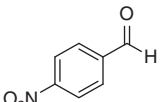
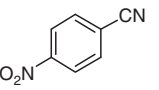
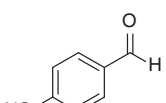
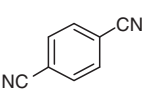
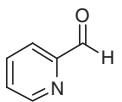
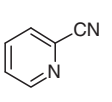
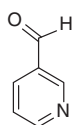
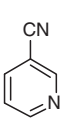
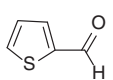
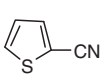
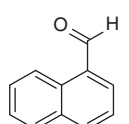
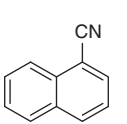
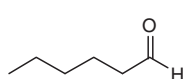
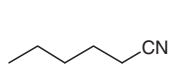
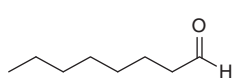
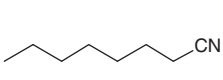
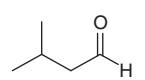
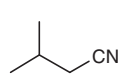
**Table 4. Direct conversion of various aldehydes into nitriles in the presence of HAP@AEPH<sub>2</sub>-SO<sub>3</sub>H nanocatalyst under optimized reaction conditions**



Entry	Aldehyde	Product	Time [min]	Isolated yield [%]
1			120	75
2			45	96
3			90	92
4			45	98
5			90	92
6			45	98
7			60	95
8			120	85
9			100	90
10			60	97
11			120	88

(Continued)

Table 4. (Continued)

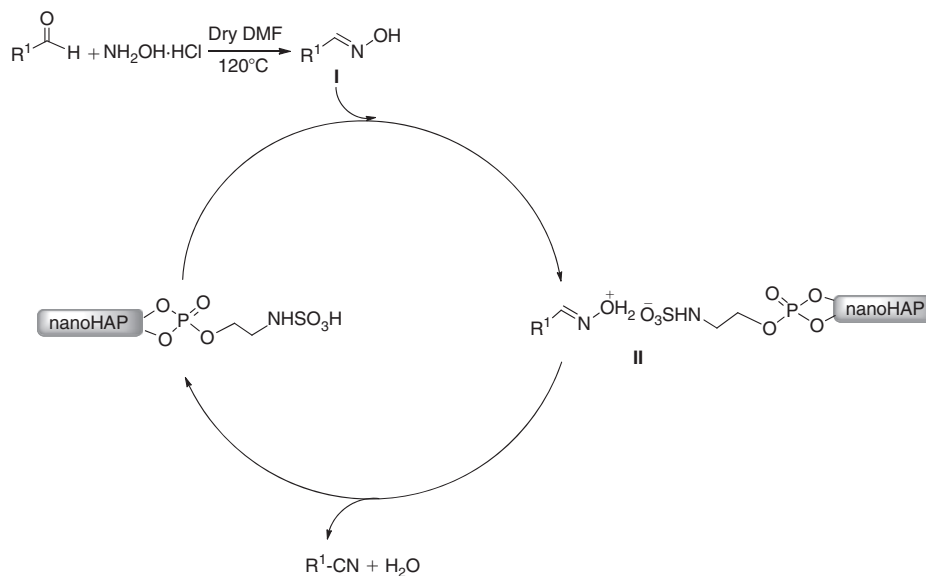
Entry	Aldehyde	Product	Time [min]	Isolated yield [%]
12			180	80
13			120	88
14			180	70
15			120	72
16			180	75
17			120	90
18			120	85
19			120	85
20			100	95
21			120	80
22			180	75

admirable yields but in longer reaction times due to the electron withdrawing effect of the heteroatom on the aromatic ring (Table 4, entries 16–18).

The catalyst was also efficient in the conversion of 1-naphthylaldehyde to the corresponding product (Table 4, entry 19). In addition, when the aliphatic aldehydes such as hexanal, octanal, and 3-methylbutanal were examined, the reactions proceeded smoothly and produced the corresponding nitriles in good yields (Table 4, entries 20–22). These results demonstrated the superior properties of HAP@AEPH<sub>2</sub>-SO<sub>3</sub>H as

an efficient solid acid nanocatalyst for direct synthesis of nitriles from aldehydes with hydroxylamine hydrochloride.

All reactions were monitored by TLC, and there is substantial evidence to confirm the structures of the synthesized nitriles. For this purpose, all purified products were characterized by comparison of their melting points, and FT-IR and mass spectra with those of authentic samples. In the FT-IR spectrum, a strong sharp absorption band at 2260–2200 cm<sup>-1</sup> was assigned to the CN group of nitriles. The molecular ion peaks (M<sup>+</sup>) observed in the mass spectra were in agreement with the expected molecular



**Scheme 2.** Proposed mechanism for direct preparation of nitriles from aldehydes and hydroxylamine hydrochloride in the presence of HAP@AEPH<sub>2</sub>-SO<sub>3</sub>H nanocatalyst.

weights. The melting points of the synthesized products also agree with the literature values. Likewise, the selected compounds were further identified by <sup>1</sup>H and <sup>13</sup>C NMR spectroscopy. In the <sup>13</sup>C NMR spectrum, a signal at around 118 ppm is assigned to the quaternary carbon of nitrile.

On the basis of the above results, and also in accordance with previous literature reports,<sup>[28,29b]</sup> a plausible mechanism is proposed as shown in Scheme 2. It is seen that the reaction proceeds via the aldoxime (I), which is formed by carrying out the reaction of aldehyde and hydroxylamine hydrochloride in dry DMF at 120°C.<sup>[29]</sup> This idea is supported by performing the reaction in the absence of catalyst (Table 3, entry 1). Afterwards in acidic media, dehydration of the aldoxime leads to formation of a nitrile, which is promoted by the protonation of the hydroxy group using a solid acid catalyst converting this moiety to a better leaving group. The solid acid nanocatalyst then re-enters the catalytic cycle by providing the active sites for further turnovers.

Recycling of the acid catalyst is an important process from different aspects such as environmental concerns, costs of the catalyst, and its toxicity. In respect of this, the possibility of recycling the HAP@AEPH<sub>2</sub>-SO<sub>3</sub>H nanocatalyst was examined using the reaction of 4-methoxybenzaldehyde and NH<sub>2</sub>OH·HCl under the optimized conditions (Table 5). In order to regenerate the nanocatalyst, after each cycle, it was separated by centrifuge, and washed several times with EtOAc. It was then dried in an oven at 50°C and used in the next run. The results show that this catalyst can be reused five times without any significant loss in activity.

Moreover, the efficiency of this method is demonstrated by comparison of our results on direct preparation of nitriles from aldehydes and hydroxylamine hydrochloride with the results reported in the literature (Table 6). As it is evident from Table 6, HAP@AEPH<sub>2</sub>-SO<sub>3</sub>H is one of the most effective nanocatalysts for this purpose, leading to the rapid formation of 4-methoxybenzonitrile in high yield. In comparison, several of the previously reported methods suffer from long reaction times to achieve appropriate yields as well as use of strong Lewis acids, expensive and toxic metals, and tedious work-up procedures.<sup>[15,16,22,29,40]</sup>

**Table 5.** Conversion of 4-methoxybenzaldehyde into 4-methoxybenzonitrile in the presence of reused nanocatalyst<sup>A</sup>

Entry	Run	Time [min]	Isolated yield [%]
1	1	45	98
2	2	45	98
3	3	45	98
4	4	45	95
5	5	45	95

<sup>A</sup>Reaction conditions: 4-methoxybenzaldehyde (1 mmol), hydroxylamine hydrochloride (3 mmol), HAP@AEPH<sub>2</sub>-SO<sub>3</sub>H nanocatalyst (8 mol-%), dry DMF (5 mL).

## Conclusion

We attempted to expand the application of a HAP@AEPH<sub>2</sub>-SO<sub>3</sub>H nanocatalyst in organic reactions. In this sense, a new and efficient procedure for direct preparation of nitriles from aldehydes and hydroxylamine hydrochloride by the HAP@AEPH<sub>2</sub>-SO<sub>3</sub>H nanocatalyst is reported. This new approach has several superiorities versus previous reports, such as short reaction times, simple procedure, high atom economy, excellent yields, generality, and recyclability of the catalyst. In addition, this new acidic nanocatalyst can be considered as an attractive alternative to harmful corrosive acids. For instance, its reusability with consistent activity for at least five cycles is also established, which indicates that, liquid acids or other solid acid catalysts can be substituted by HAP@AEPH<sub>2</sub>-SO<sub>3</sub>H as a green solid acid nanocatalyst.

## Experimental

### General

The purity determinations of the products were accomplished using TLC on silica gel polygram STL G/UV 254 plates. The melting points of products were determined with an Electro-thermal type 9100 melting point apparatus. FT-IR spectra were

**Table 6. Comparison efficiency of various catalysts in the direct conversion of 4-methoxybenzaldehyde into 4-methoxybenzotrile**

Entry	Catalyst	Amount of catalyst [g]	Solvent	Temperature [°C]	Time [h]	Yield [%]	Ref.
1	FeCl <sub>3</sub>	0.081	DMF	154	4	98	[15]
2	Graphite/MeSO <sub>2</sub> Cl	0.1	–	100	120 min	98	[16]
3	Bi(OTf) <sub>3</sub>	0.11	CH <sub>3</sub> CN	Reflux	17	95	[29]
4	CeCl <sub>3</sub> ·7H <sub>2</sub> O/KI/H <sub>2</sub> O	3 mmol	–	R.T	120 min	82	[22]
5	KF/Al <sub>2</sub> O <sub>3</sub>	7.25	DMF	100	7	91	[40]
6	HAP@AEPH <sub>2</sub> -SO <sub>3</sub> H	0.08	DMF	120	45 min	98	Present study

recorded on pressed KBr pellets using an AVATAR 370 FT-IR spectrometer (Thermo Nicolet spectrometer, USA) at room temperature in the range between 4000 and 400 cm<sup>-1</sup> with a resolution of 4 cm<sup>-1</sup>. NMR spectra were obtained with Bruker AMX 100, 300, and 400 MHz instruments in CDCl<sub>3</sub>. Elemental analyses were performed using a Thermo Finnegan Flash EA 1112 series instrument. Mass spectra were recorded with a CH7A Varianmat Bremem instrument at 70 eV electron impact ionization, in *m/z* (rel.-%). TGA and DTA analysis were performed using a Shimadzu Thermogravimetric Analyzer (TG-50) in the temperature range of 25–900°C at a heating rate of 10°C min<sup>-1</sup> under air atmosphere. SEM images were recorded using Leo 1450 VP scanning electron microscope operating at an acceleration voltage 20 kV, resolution of ~2 nm, image with a magnification of 20 to 300 000 times (LEO, Germany). TEM was performed with a Leo 912 AB microscope (Zeiss, Germany) with an accelerating voltage of 120 kV, image with a magnification of 80 to 500 000 times, equipped with a high resolution CCD Camera. The crystal structure of the catalyst was analyzed by XRD using a D8 ADVANCE Bruker diffractometer operated at 40 kV and 30 mA utilising Cu K $\alpha$  radiation ( $\lambda$  0.154 Å), at a step size of 0.040° and step time of 1.5 s. The diffraction angles ( $2\theta$ ) were scanned from 10° to 80°. BET surface area and pore size distribution were measured on a Belsorp mini II system at -196°C using N<sub>2</sub> as adsorbate. All of the products were known compounds and characterized using FT-IR spectroscopy, mass spectrometry, and comparison of their melting points with known compounds. The structure of selected products was further confirmed using <sup>1</sup>H and <sup>13</sup>C NMR spectroscopy.

#### Typical Procedure for Preparation of 4-Methoxybenzotrile

To a solution of 4-methoxybenzaldehyde (1 mmol, 0.136 g) in dry DMF (5 mL), hydroxylamine hydrochloride (3 mmol, 0.208 g) was added with stirring for 15 min at 120°C. HAP@AEPH<sub>2</sub>-SO<sub>3</sub>H nanocatalyst (8 mol-%, 0.08 g) was then added to the resultant solution. After completion of the reaction (which was monitored by TLC), cooling, and separation of the nanocatalyst by centrifugation, the reaction mixture was poured into water (10 mL). The resulting mixture was extracted with ethyl acetate (3 × 10 mL) and dried over sodium sulfate. After evaporation of the solvent, the crude product was purified by thin-layer chromatography using *n*-hexane/ethyl acetate (4 : 1) as eluent to afford 4-methoxybenzotrile (0.130 g, 98 %).

#### Preparation of NanoHAP Functionalized with AEPH<sub>2</sub> (HAP@AEPH<sub>2</sub>)

To a solution of Ca(NO<sub>3</sub>)<sub>2</sub>·4H<sub>2</sub>O (50 mL, 1.08 M, at pH adjusted to 10 with NH<sub>4</sub>OH) in a three-necked 500 mL round-bottomed flask equipped with a condenser, argon gas inlet

tube, and dropping funnel, a solution of (NH<sub>4</sub>)<sub>2</sub>HPO<sub>4</sub> (50 mL, 0.65 M at pH adjusted to 10 with NH<sub>4</sub>OH) was added at 90°C with stirring. AEPH<sub>2</sub> (0.8 g, 5 mmol) was added to the resulting suspension. The precipitate was maintained in contact with the reaction solution for 5 h at 90°C under stirring. Then suspension was centrifuged at 250000 g for 10 min and repeatedly washed with CO<sub>2</sub>-free distilled water (3 × 20 mL). The product (nanoHAP functionalized with AEPH<sub>2</sub>) was dried at 50°C overnight.<sup>[27,28]</sup>

#### Preparation of HAP@AEPH<sub>2</sub>-SO<sub>3</sub>H

To a magnetically stirred mixture of HAP@AEPH<sub>2</sub> (1 g) in 20 mL of dry dichloromethane, 0.5 mL (0.75 mmol) of chlorosulfuric acid was added drop by drop at room temperature. After 20 min the suspension was filtered and washed with 20 mL of dichloromethane and dried at room temperature to afford HAP@AEPH<sub>2</sub>-SO<sub>3</sub>H as a white powder.<sup>[27,28]</sup>

#### Catalyst Product Characterization

Benzotrile (Table 4, Entry 1). Oil (Lit.<sup>[41]</sup> oil).  $\nu_{\max}$  (neat)/cm<sup>-1</sup> 3066, 2228 (CN) 1599, 1489, 1447, 1287, 1177, 1070, 1025, 927, 759, 687, 547.  $\delta_{\text{H}}$  (CDCl<sub>3</sub>, 400 MHz) 7.66–7.59 (m, 3H, Ar), 7.50–7.46 (m, 2H, Ar).  $\delta_{\text{C}}$  (CDCl<sub>3</sub>, 100 MHz) 132.7, 132.0, 129.0, 118.7, 112.4. *m/z* (ESI) 103 (5 %, M<sup>+</sup>).

4-Hydroxybenzotrile (Table 4, Entry 2). Mp 108–110°C (Lit.<sup>[20]</sup> 111–112°C).  $\nu_{\max}$  (KBr)/cm<sup>-1</sup> 3310, 2233 (CN), 1907, 1785, 1612, 1586, 1510, 1443, 1377, 1284, 1222, 1164, 1103, 967, 839, 701, 669, 547. *m/z* (ESI) 119 (91 %, M<sup>+</sup>).

2-Hydroxybenzotrile (Table 4, Entry 3). Mp 92–94°C (Lit.<sup>[42]</sup> 94°C).  $\nu_{\max}$  (KBr)/cm<sup>-1</sup> 3231, 3068, 2966, 2864, 2729, 2602, 2508, 2467, 2345, 2239 (CN), 1604, 1505, 1458, 1369, 1306, 1269, 1239, 1102, 1037, 947, 848, 769, 754, 731, 687, 567, 496, 465. *m/z* (ESI) 119 (95 %, M<sup>+</sup>).

4-Methoxybenzotrile (Table 4, Entry 4). Mp 56–58°C (Lit.<sup>[43]</sup> 58–59°C).  $\nu_{\max}$  (KBr)/cm<sup>-1</sup> 3050, 2931, 2847, 2213 (CN), 1604, 1506, 1454, 1303, 1256, 1170, 1020, 828, 678, 546, 406. *m/z* (ESI) 148 (23 %, M<sup>+</sup>).

3-Methoxybenzotrile (Table 4, Entry 5). Oil (Lit.<sup>[44]</sup> oil).  $\nu_{\max}$  (neat)/cm<sup>-1</sup> 3076, 2970, 2944, 2835, 2230 (CN), 1764, 1737, 1595, 1580, 1486, 1465, 1428, 1373, 1327, 1289, 1246, 1164, 1145, 1045, 912, 873, 855, 788, 682, 596, 534, 475. *m/z* (ESI) 148 (31 %, M<sup>+</sup>).

4-Ethoxybenzotrile (Table 4, Entry 6). Mp 51–53°C (Lit.<sup>[45]</sup> 51–53°C).  $\nu_{\max}$  (KBr)/cm<sup>-1</sup> 3071, 2995, 2980, 2939, 2896, 2219 (CN), 1604, 1573, 1506, 1475, 1392, 1301, 1259, 1172, 1109, 1039, 918, 845, 809, 707, 547. *m/z* (ESI) 147 (10 %, M<sup>+</sup>).

4-Methylbenzotrile (Table 4, Entry 7). Mp 26–27°C (Lit.<sup>[46]</sup> 26–28°C).  $\nu_{\max}$  (neat)/cm<sup>-1</sup> 3041, 2926, 2861, 2227 (CN),

1918, 1739, 1608, 1507, 1452, 1379, 1245, 1177, 1113, 1047, 957, 819, 703, 547, 438 cm<sup>-1</sup>.  $\delta_{\text{H}}$  (CDCl<sub>3</sub>, 400 MHz) 7.53 (d, *J* 8.2, 2H, Ar), 7.27 (d, *J* 8.2, 2H, Ar), 2.42 (s, 3H, CH<sub>3</sub>).  $\delta_{\text{C}}$  (CDCl<sub>3</sub>, 100 MHz) 143.6, 131.9, 129.7, 119.1, 109.2, 21.7. *m/z* (ESI) 117 (19%, M<sup>+</sup>).

2-Methylbenzonitrile (Table 4, Entry 8). Oil (Lit.<sup>[47]</sup> oil).  $\nu_{\text{max}}$  (neat)/cm<sup>-1</sup> 3064, 3038, 2962, 2925, 2865, 2227 (CN), 1608, 1508, 1450, 1412, 1382, 1177, 1120, 1041, 955, 817, 710, 669, 546, 439. *m/z* (ESI) 117 (10%, M<sup>+</sup>).

4-Isopropylbenzonitrile (Table 4, Entry 9). Oil (Lit.<sup>[20]</sup> oil).  $\nu_{\text{max}}$  (neat)/cm<sup>-1</sup> 3078, 2965, 2929, 2872, 2228 (CN), 1737, 1684, 1606, 1503, 1460, 1366, 1244, 1197, 1100, 1053, 1018, 838, 761, 695, 566. *m/z* (ESI) 145 (17%, M<sup>+</sup>).

4-(Dimethylamino)benzonitrile (Table 4, Entry 10). Mp 70–72°C (Lit.<sup>[48]</sup> 72–75°C).  $\nu_{\text{max}}$  (KBr)/cm<sup>-1</sup> 2917, 2864, 2814, 2207 (CN), 1606, 1524, 1446, 1368, 1227, 1171, 1125, 1066, 938, 817, 645, 544. *m/z* (ESI) 146 (95%, M<sup>+</sup>).

4-Chlorobenzonitrile (Table 4, Entry 11). Mp 89–91°C (Lit.<sup>[43]</sup> 92°C).  $\nu_{\text{max}}$  (KBr)/cm<sup>-1</sup> 3086, 3043, 2974, 2218 (CN), 1909, 1783, 1662, 1584, 1481, 1393, 1267, 1180, 1083, 1009, 826, 703, 580, 539.  $\delta_{\text{H}}$  (CDCl<sub>3</sub>, 400 MHz) 7.61 (d, *J* 8.6, 2H, Ar), 7.47 (d, *J* 8.6, 2H, Ar).  $\delta_{\text{C}}$  (CDCl<sub>3</sub>, 100 MHz) 139.5, 133.3, 129.6, 117.9, 110.7. *m/z* (ESI) 137 (85%, M<sup>+</sup>).

2,6-Dichlorobenzonitrile (Table 4, Entry 12). Mp 140–143°C (Lit.<sup>[49]</sup> 142–145°C).  $\nu_{\text{max}}$  (KBr)/cm<sup>-1</sup> 3145, 3090, 2230 (CN), 1748, 1706, 1571, 1509, 1430, 1228, 1196, 1102, 782, 714, 547. *m/z* (ESI) 172 (92%, M<sup>+</sup>).

4-Bromobenzonitrile (Table 4, Entry 13). Mp 112–113°C (Lit.<sup>[46]</sup> 113–115°C).  $\nu_{\text{max}}$  (KBr)/cm<sup>-1</sup> 3106, 3060, 2991, 2933, 2857, 2227 (CN), 1603, 1527, 1437, 1346, 1288, 1190, 1103, 1010, 858, 749, 679, 540. *m/z* (ESI) 182 (100%, M<sup>+</sup>).

4-Nitrobenzonitrile (Table 4, Entry 14). Mp 146–148°C (Lit.<sup>[50]</sup> 149°C).  $\nu_{\text{max}}$  (KBr)/cm<sup>-1</sup> 3059, 2963, 2926, 2855, 2224 (CN), 1733, 1687, 1584, 1503, 1380, 1343, 1240, 1157, 1062, 1013, 961, 806, 770, 693, 587, 457.  $\delta_{\text{H}}$  (CDCl<sub>3</sub>, 400 MHz) 8.37 (d, *J* 8.8, 2H, Ar), 7.91 (d, *J* 8.8, 2H, Ar).  $\delta_{\text{C}}$  (CDCl<sub>3</sub>, 100 MHz) 150.0, 133.4, 124.2, 118.3, 116.8. *m/z* (ESI) 148 (45%, M<sup>+</sup>).

Terephthalonitrile (Table 4, Entry 15). Mp 218–220°C (Lit.<sup>[17]</sup> 219–220°C).  $\nu_{\text{max}}$  (KBr)/cm<sup>-1</sup> 3096, 3050, 2962, 2924, 2854, 2230 (CN), 1941, 1809, 1692, 1500, 1402, 1276, 1198, 1025, 844, 641, 561.  $\delta_{\text{H}}$  (CDCl<sub>3</sub>, 400 MHz) 7.81 (s, 4H, Ar).  $\delta_{\text{C}}$  (CDCl<sub>3</sub>, 100 MHz) 132.8, 117.0, 116.7. *m/z* (ESI) 128 (5%, M<sup>+</sup>).

2-Cyanopyridine (Table 4, Entry 16). Oil (Lit.<sup>[41]</sup> oil).  $\nu_{\text{max}}$  (neat)/cm<sup>-1</sup> 2917, 2864, 2814, 2207 (CN), 1606, 1524, 1446, 1368, 1227, 1171, 1125, 1066, 938, 817, 645, 544.  $\delta_{\text{H}}$  (400 MHz, CDCl<sub>3</sub>) 7.35 (s, 1H, Py), 7.74 (s, 1H, Py), 7.844 (d, *J* 6.4, 1H, Py), 8.51 (s, 1H, Py). *m/z* (ESI) 104 (12%, M<sup>+</sup>).

3-Cyanopyridine (Table 4, Entry 17). Mp 46–50°C (Lit.<sup>[51]</sup> 48–51°C).  $\nu_{\text{max}}$  (KBr)/cm<sup>-1</sup> 3141, 3083, 3026, 2990 (CN), 2239, 1973, 1718, 1591, 1543, 1493, 1414, 1331, 1236, 1206, 1111, 1081, 987, 827, 775, 559. *m/z* (ESI) 104 (12%, M<sup>+</sup>).

Thiophen-2-carbonitrile (Table 4, Entry 18). Oil (Lit.<sup>[52]</sup> oil).  $\nu_{\text{max}}$  (neat)/cm<sup>-1</sup> 3109, 3098, 2221 (CN), 1413, 1349, 1232, 1157, 1077, 1040, 856, 719, 567, 524, 486. *m/z* (ESI) 109 (30%, M<sup>+</sup>).

1-Naphthonitrile (Table 4, Entry 19). Mp 32–34°C (Lit.<sup>[16]</sup> 34°C).  $\nu_{\text{max}}$  (neat)/cm<sup>-1</sup> 3058, 2926, 2847, 2222 (CN), 1625, 1586, 1508, 1375, 1342, 1242, 1162, 1047, 863, 803, 772, 689, 572, 453.  $\delta_{\text{H}}$  (CDCl<sub>3</sub>, 400 MHz) 8.21 (d, *J* 8.0, 1H, Ar), 8.05 (d, *J* 8.0, 1H, Ar), 7.92–7.88 (m, 2H, Ar), 7.69–7.66 (m, 1H, Ar), 7.62–7.758 (m, 1H, Ar), 7.52–7.48 (m, 1H, Ar).  $\delta_{\text{C}}$  (CDCl<sub>3</sub>,

100 MHz) 133.2, 132.8, 132.5, 132.3, 128.6, 128.5, 127.5, 125.0, 124.8, 117.7, 110.1. *m/z* (ESI) 153 (100%, M<sup>+</sup>).

Hexanenitrile (Table 4, Entry 20). Oil (Lit.<sup>[53]</sup> oil).  $\delta_{\text{H}}$  (CDCl<sub>3</sub>, 300 MHz) 2.34 (t, *J* 12.0, 2H, CH<sub>2</sub>), 1.72–1.62 (m, 2H, CH<sub>2</sub>), 1.49–1.32 (m, 4H, CH<sub>2</sub>), 0.93 (t, *J* 12.0, 3H, CH<sub>3</sub>).  $\delta_{\text{C}}$  (CDCl<sub>3</sub>, 75 MHz) 119.7, 30.6, 24.9, 21.7, 16.9, 13.5.

Octanenitrile (Table 4, Entry 21). Oil (Lit.<sup>[54]</sup> oil).  $\nu_{\text{max}}$  (neat)/cm<sup>-1</sup> 2962, 2930, 2859, 2246 (CN), 1462, 1427, 1377, 1119, 723. *m/z* (ESI) 125 (2%, M<sup>+</sup>).

3-Methylbutanenitrile (Table 4, Entry 22). Oil (Lit.<sup>[55]</sup> oil).  $\nu_{\text{max}}$  (neat)/cm<sup>-1</sup> 3648, 2966, 2933, 2876, 2246, 1467, 1425, 1391, 1342, 1282, 1171, 1114, 935, 891, 820. *m/z* (ESI) 83 (3%, M<sup>+</sup>).

## Supplementary Material

Details of analysis of nitrile derivatives are available on the Journal's website.

## Acknowledgements

The authors gratefully acknowledge the partial support of this study by Ferdowsi University of Mashhad Research Council (grant no. p/3/38854).

## References

- (a) R. C. Larock, *Comprehensive Organic Transformations* **1989** (VCH: New York, NY).  
(b) C. Grundmann, in *Houben-Weyl: Methodender Organischen Chemie* (Ed. J. Falbe) **1985**, pp. 1313–1527 (Georg Thieme: Stuttgart).
- (a) C. J. Moody, K. J. Doyle, *Prog. Heterocycl. Chem.* **1997**, *9*, 1. doi:10.1016/S0959-6380(97)80003-7  
(b) P. C. Ducept, S. P. Marsden, *Synlett* **2000**, 692.
- (a) X. H. Gu, X. Z. Wan, B. Jiang, *Bioorg. Med. Chem. Lett.* **1999**, *9*, 569. doi:10.1016/S0960-894X(99)00037-2  
(b) M. Chihiro, H. Nagamoto, I. Takemura, K. Kitano, H. Komatsu, K. Sekiguchi, F. Tabusa, T. Mori, M. Tominaga, Y. Yabuuchi, *J. Med. Chem.* **1995**, *38*, 353. doi:10.1021/JM00002A017
- (a) S. J. Wittenberger, B. G. Donner, *J. Org. Chem.* **1993**, *58*, 4139. doi:10.1021/JO00067A058  
(b) T. R. Bailey, G. D. Diana, P. J. Kowalczyk, V. Akullian, M. A. Eissenstat, D. Cutcliffe, J. P. Mallamo, P. M. Carabateas, D. C. Pevear, *J. Med. Chem.* **1992**, *35*, 4628. doi:10.1021/JM00102A017  
(c) P. K. Kadaba, *Synthesis* **1973**, 71.
- G. K. Jnaneshwara, V. H. Deshpande, M. Lalithambika, T. Ravindranathan, A. V. Bedekar, *Tetrahedron Lett.* **1998**, *39*, 459. doi:10.1016/S0040-4039(97)10575-5
- R. F. Smith, J. A. Albright, A. M. Waring, *J. Org. Chem.* **1966**, *31*, 4100. doi:10.1021/JO01350A053
- M. E. Fabiani, *Drug News Perspect.* **1999**, *12*, 207.
- L. Bini, C. Muller, J. Wilting, L. Chrzanowski, A. L. Spek, D. Vogt, *J. Am. Chem. Soc.* **2007**, *129*, 12622. doi:10.1021/JA074922E
- (a) T. Sandmeyer, *Ber. Dtsch. Chem. Ges.* **1885**, *18*, 1946.  
(b) T. Sandmeyer, *Ber. Dtsch. Chem. Ges.* **1885**, *18*, 1492. doi:10.1002/CBER.188501801322  
(c) T. Sandmeyer, *Ber. Dtsch. Chem. Ges.* **1884**, *17*, 2650. doi:10.1002/CBER.188401702202
- (a) K. W. Rosenmund, E. Struck, *Ber. Dtsch. Chem. Ges.* **1919**, *52*, 1749. doi:10.1002/CBER.19190520840  
(b) J. Lindley, *Tetrahedron* **1984**, *40*, 1433. doi:10.1016/S0040-4020(01)91791-0
- L. Friedman, H. Shechter, *J. Org. Chem.* **1960**, *25*, 877. doi:10.1021/JO01076A001
- (a) S. H. Khezri, N. Azimi, M. Mohammed-Vali, B. Eftekhari-Sis, M. M. Hashemi, M. H. Baniyasi, F. Teimouric, *ARKIVOC* **2007**, *15*, 162.  
(b) R. S. Glass, R. C. Hoy, *Tetrahedron Lett.* **1976**, *17*, 1781. doi:10.1016/S0040-4039(00)93781-X

- (c) K. Nishiyama, M. Oba, A. Watanabe, *Tetrahedron* **1987**, *43*, 693. doi:10.1016/S0040-4020(01)90003-1
- [13] H. Veisi, *Synthesis* **2010**, 2631. doi:10.1055/S-0029-1218827
- [14] H. Sharghi, M. Hosseini Sarvari, *Tetrahedron* **2002**, *58*, 10323. doi:10.1016/S0040-4020(02)01417-5
- [15] P. Ghosh, R. Subba, *Tetrahedron Lett.* **2013**, *54*, 4885. doi:10.1016/J.TETLET.2013.06.134
- [16] H. Sharghi, M. Hosseini Sarvari, *Synthesis* **2003**, 243. doi:10.1055/S-2003-36830
- [17] M. B. Madhusudana Reddy, M. A. Pasha, *Chin. Chem. Lett.* **2010**, *21*, 1025. doi:10.1016/J.CCLET.2010.05.004
- [18] V. K. Das, S. N. Harsh, N. Karak, *Tetrahedron Lett.* **2016**, *57*, 549. doi:10.1016/J.TETLET.2015.12.083
- [19] G. C. Nandi, K. K. Laali, *Tetrahedron Lett.* **2013**, *54*, 2177. doi:10.1016/J.TETLET.2013.02.051
- [20] M. Sridhar, M. K. K. Reddy, V. V. Sairam, J. Raveendra, K. R. Godala, C. Narsaiah, B. C. Ramanaiah, C. S. Reddy, *Tetrahedron Lett.* **2012**, *53*, 3421. doi:10.1016/J.TETLET.2012.04.057
- [21] B. S. Anandakumar, M. B. M. Reddy, C. N. Tharamani, M. A. Pasha, G. T. Chandrappa, *Chin. J. Catal.* **2013**, *34*, 704. doi:10.1016/S1872-2067(11)60503-2
- [22] M. Hajjami, A. Ghorbani-Choghamarani, M. A. Zolfigol, F. Gholamian, *Chin. Chem. Lett.* **2012**, *23*, 1323. doi:10.1016/J.CCLET.2012.10.006
- [23] B. V. Rokade, K. R. Prabhu, *J. Org. Chem.* **2012**, *77*, 5364. doi:10.1021/JO3008258
- [24] Q. Chen, C. Fang, Z. H. Shen, M. Li, *Electrochem. Commun.* **2016**, *64*, 51. doi:10.1016/J.ELECOM.2016.01.011
- [25] (a) P. Gupta, S. Paul, *Catal. Today* **2014**, *236*, 153. doi:10.1016/J.CATTOD.2014.04.010  
(b) R. A. Sheldon, in *Fine Chemicals through Heterogeneous Catalysis* (Ed. H. V. Bekkum) **2001**, pp. 1–11 (Wiley-VCH: Weinheim).
- [26] (a) K. Niknam, D. Saberi, M. Nouri Sefat, *Tetrahedron Lett.* **2010**, *51*, 2959. doi:10.1016/J.TETLET.2010.03.093  
(b) D. S. Bose, A. V. Narsaiah, *Tetrahedron Lett.* **1998**, *39*, 6533. doi:10.1016/S0040-4039(98)01358-6
- [27] M. Zarghani, B. Akhlaghinia, *RSC Adv.* **2015**, *5*, 87769. doi:10.1039/C5RA16236J
- [28] N. Yousefi Siavashi, B. Akhlaghinia, M. Zarghani, *Res. Chem. Intermed.* **2016**, in press. doi:10.1007/S11164-015-2404-8
- [29] (a) N. Razavi, B. Akhlaghinia, *RSC Adv.* **2015**, *5*, 12372. doi:10.1039/C4RA15148H  
(b) M. Zarghani, B. Akhlaghinia, *Appl. Organomet. Chem.* **2015**, *29*, 683. doi:10.1002/AOC.3351  
(c) S. S. E. Ghodsinia, B. Akhlaghinia, *RSC Adv.* **2015**, *5*, 49849. doi:10.1039/C5RA08147E  
(d) Z. Zareie, B. Akhlaghinia, *Chem. Pap.* **2015**, *69*, 1421.  
(e) N. Razavi, B. Akhlaghinia, *New J. Chem.* **2016**, *40*, 447. doi:10.1039/C5NJ02123E  
(f) R. Jahanshahi, B. Akhlaghinia, *RSC Adv.* **2015**, *5*, 104087. doi:10.1039/C5RA21481E
- [30] M. G. Ma, Y. J. Zhu, J. Chang, *J. Phys. Chem. B* **2006**, *110*, 14226. doi:10.1021/JP061738R
- [31] Y. Daniels, N. Lyczko, A. Nzihou, S. D. Alexandratos, *Ind. Eng. Chem. Res.* **2015**, *54*, 585. doi:10.1021/IE504181Z
- [32] A. Badii, H. Goldooz, G. Mohammadi Ziarani, A. Abbasi, *J. Colloid Interface Sci.* **2011**, *357*, 63. doi:10.1016/J.JCIS.2011.01.049
- [33] M. Sheykhan, L. Ma'mani, A. Ebrahimi, A. Heydari, *J. Mol. Catal. Chem.* **2011**, *335*, 253. doi:10.1016/J.MOLCATA.2010.12.004
- [34] A. Z. Alshemary, Y. Goh, M. Akram, I. R. Razali, M. A. Kadir, R. Hussain, *Mater. Res. Bull.* **2013**, *48*, 2106. doi:10.1016/J.MATER.RESBULL.2013.02.015
- [35] (a) F. Mohandes, M. Salavati-Niasari, *Mater. Sci. Eng. C* **2014**, *40*, 288. doi:10.1016/J.MSEC.2014.04.008  
(b) G. E. Poinern, R. K. Brundavanam, N. Mondinos, Z. T. Jiang, *Ultrason. Sonochem.* **2009**, *16*, 469. doi:10.1016/J.ULTSONCH.2009.01.007
- [36] G. Wang, Y. Zhao, J. Tan, S. Zhu, K. Zhou, *Trans. Nonferrous Met. Soc. China.* **2015**, *25*, 490. doi:10.1016/S1003-6326(15)63629-9
- [37] Y.-R. Jiang, F.-H. Sun, X.-Y. Zhou, W.-B. Kong, X.-Y. Xie, *Chin. Chem. Lett.* **2015**, *26*, 1121. doi:10.1016/J.CCLET.2015.04.035
- [38] N. Ahmed, Z. N. Siddiqui, *J. Mol. Catal. Chem.* **2014**, *394*, 232. doi:10.1016/J.MOLCATA.2014.07.015
- [39] L. El-Hammari, H. Marroun, A. Laghzizil, A. Saouiabi, C. Roux, J. Livage, T. Coradin, *J. Solid State Chem.* **2008**, *181*, 848. doi:10.1016/J.JSSC.2008.01.030
- [40] B. Movassagh, S. Shokri, *Tetrahedron Lett.* **2005**, *46*, 6923. doi:10.1016/J.TETLET.2005.08.007
- [41] N. Coskun, *Synth. Commun.* **2004**, *34*, 1625. doi:10.1081/SCC-120030750
- [42] X. C. Wang, L. Li, Z. J. Quan, H. P. Gong, H. L. Ye, X. F. Cao, *Chin. Chem. Lett.* **2009**, *20*, 651. doi:10.1016/J.CCLET.2009.02.004
- [43] U. Patil, A. Kuwar, A. Nikum, K. Desale, P. Mahulikar, *Int. J. Chem. Tech. Res.* **2013**, *5*, 24.
- [44] H. S. Kim, S. H. Kim, J. N. Kim, *Tetrahedron Lett.* **2009**, *50*, 1717. doi:10.1016/J.TETLET.2009.01.150
- [45] X. Wei, D. Quansheng, C. Jiuxi, D. Jinchang, W. Huayue, *J. Chem. Res.* **2010**, *7*, 395.
- [46] A. Ghorbani-Choghamarani, M. A. Zolfigol, M. Hajjami, S. Sardari, *Synth. Commun.* **2013**, *43*, 52. doi:10.1080/00397911.2011.591035
- [47] N. Jiang, A. J. Ragauskas, *Tetrahedron Lett.* **2010**, *51*, 4479. doi:10.1016/J.TETLET.2010.06.079
- [48] N. D. Kokare, D. B. Shinde, *Monatsh. Chem.* **2009**, *140*, 185. doi:10.1007/S00706-008-0058-6
- [49] N. Lingaiah, R. Narender, *Synth. Commun.* **2002**, *32*, 2391. doi:10.1081/SCC-120006011
- [50] A. R. Sardarian, Z. Shahsavari Fard, H. R. Shahsavari, Z. Ebrahimi, *Tetrahedron Lett.* **2007**, *48*, 2639. doi:10.1016/J.TETLET.2007.01.120
- [51] M. Heravi, S. Sadjadi, R. Hekmatshoar, H. Oskooie, F. Bamoharram, *Chin. J. Chem.* **2009**, *27*, 607. doi:10.1002/CJOC.200990099
- [52] N. S. Nandurkar, B. M. Bhanage, *Tetrahedron* **2008**, *64*, 3655. doi:10.1016/J.TET.2008.02.038
- [53] M. Dreisbach, *Ind. Eng. Chem.* **1949**, *41*, 2876.
- [54] J. A. Campbell, G. McDougald, H. McNab, L. V. C. Rees, R. G. Tyas, *Synthesis* **2007**, 3179.
- [55] T. Delcourt, *J. Chim. Phys.* **1934**, *31*, 110.